

Article

Hydrologic Response of Climate Change in the Source Region of the Yangtze River, Based on Water Balance Analysis

Yiheng Du ^{1,*}, Ronny Berndtsson ^{1,2}, Dong An ¹, Linus Zhang ¹, Zhenchun Hao ³ and Feifei Yuan ³

¹ Division of Water Resources Engineering, Lund University, SE 22100 Lund, Sweden; ronny.berndtsson@tvrl.lth.se (R.B.); dong.an@tvrl.lth.se (D.A.); linus.zhang@tvrl.lth.se (L.Z.)

² Center for Middle Eastern Studies, Lund University, SE 22100 Lund, Sweden

³ State Key Laboratory of Hydrology, Water Resources, and Hydraulic Engineering, Hohai University, Nanjing 221000, China; hzchun@hhu.edu.cn (Z.H.); feifei.yuan@tvrl.lth.se (F.Y.)

* Correspondence: yiheng.du@tvrl.lth.se; Tel.: +46-73-106-1458

Academic Editor: Gordon Huang

Received: 5 December 2016; Accepted: 8 February 2017; Published: 13 February 2017

Abstract: Due to the large amount of water resources stored in glaciers, permafrost, and lakes, the source region of the Yangtze River (SRYR) is of great importance for the overall basin water flow. For this purpose, a state of art review and calculations were made for the period 1957–2013 using observed hydrological and meteorological data with a water balance approach. Actual evapotranspiration was calculated and validated by empirical formulas. Water storage change analysis was conducted with uncertainty boundaries using a 10-year moving window. Results show that temperature, precipitation, and actual evapotranspiration in the SRYR increased by 0.34 °C, 11.4 mm, and 7.6 mm per decade, respectively (significant at 0.05 probability level). Runoff appears to have increased at a rate of 3.3 mm per decade. The SRYR water storage in total has not changed significantly during the period, although the moving average is mostly below zero. Based on the water balance equation, the increase in calculated evapotranspiration is mainly due to the significantly increasing temperature. This in combination with increasing precipitation leads to a relatively stable water storage during the study period. Correlation analyses show that precipitation dominates runoff during the warm season (May to October), while temperature anomalies dominate the runoff during the cold season (November to April). The influence of temperature on runoff seems to enhance during the winter period.

Keywords: source region of the Yangtze River; climate change; water balance; uncertainty propagation; correlation analysis

1. Introduction

Over the past century, global climate has undergone a significant warming [1]. Due to its great importance for water resources supply, climate change in the Tibet Plateau and its impacts are of great interest [2–4]. The average warming in the Tibet Plateau during the past 50 years has been stronger than in other regions on the same latitude [5]. The source region of the Yangtze River (SRYR), the longest river in China, is located in the center of the Tibet Plateau. Due to the high elevation and low temperature in the region, a huge water volume is retained in glaciers, permafrost, and lakes. The water in glaciers only represents about 88.8 km³ [6]. As the hydrological cycle of the SRYR is similar to that of Antarctica, with comparably small inflow and outflow but a large quantity of stored water, it is important to study water balance changes due to climate change.

To improve the understanding of the influence of climate change on the SRYR, much effort has been devoted to analyze the trend in runoff and its influencing climatic factors. Due to different length of data records, seemingly contradictory trends for precipitation and runoff have been found [7–9]. Only temperature has been confirmed to increase significantly in the SRYR [10–12]. For water storage change, some researchers have emphasized the change of certain components, such as glaciers [6,13], permafrost, lakes, or groundwater [14–17]. Since runoff directly influences societal safety and food security, special attention has been given to runoff and climatic variables [12]. The impact of increasing temperature on runoff volume is a major worldwide research topic [18–20]. As temperature has a significant effect on water cycle components such as evaporation and water storage in glaciers and permafrost, this will lead to complex changes in cold region basins such as the SRYR.

In view of the above, this paper aims at analyzing the trend of water balance components to estimate the effects of climate change. The aim of the paper is to perform an analysis of the hydro-climatic components of the SRYR using the latest data, to perform water storage calculations with uncertainty analysis, and to analyze effects of temperature and precipitation on runoff. The paper closes with a discussion on practical applications of the results and urgent research needs for the area.

2. Study Area and Methods

2.1. Study Area and Data

The source region of the Yangtze River (SRYR) is located in the hinterland of the Qinghai-Tibet plateau, which refers to the basin above the Zhimenda runoff station (Figure 1). The region has an average elevation of over 4500 m amsl ($90^{\circ}33'–95^{\circ}20'$ E, $32^{\circ}26'–35^{\circ}46'$ N) and the basin area is 13.77×10^4 km 2 . The SRYR consists of three sub-basins, namely Chumar (north source), Tuotuohe (middle source), and Dangqu (south source) River. These three sources collect more than 200 smaller river tributaries that discharge from Zhimenda into the lower section of the Tongtian River. Due to the harsh climatic conditions, only about 15,000 people live in the area (0.09 person per km 2). Thus, the river system is mainly pristine [21]. As a result, the direct human impact on the hydrological processes is small.

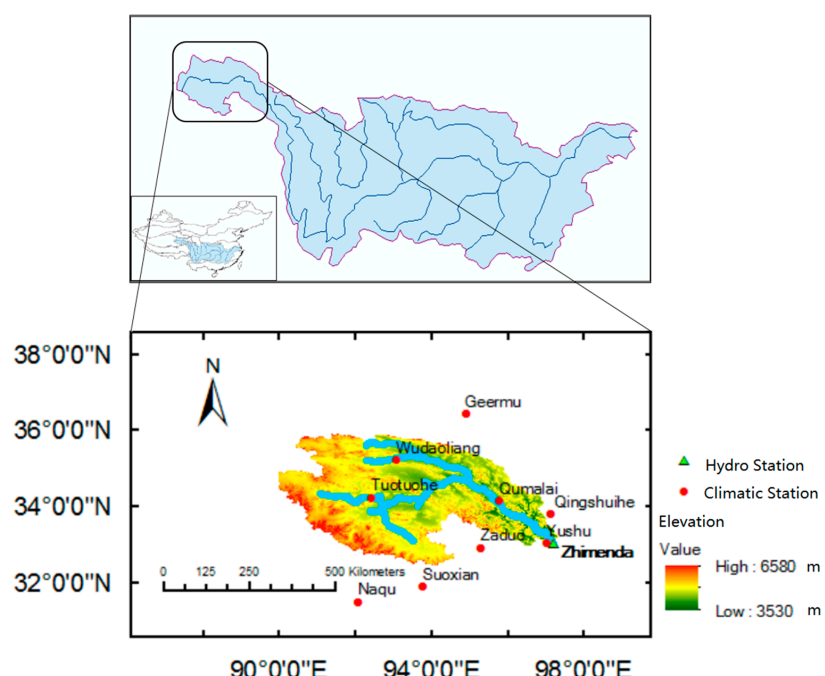


Figure 1. The location of the source region of the Yangtze River with one hydrological and nine climatological observation stations.

Thiessen polygons were created based on the locations of the nine climatological stations and areal weights were derived. In total, four stations inside and five stations outside the catchment border (with effective area in Thiessen polygons) were used to analyze the distribution and trend of water balance components (1957–2013). Monthly observed temperature and precipitation were taken from the data-sharing website of the National Meteorological Information Center, China (<http://data.cma.cn/>). Monthly discharge data of the Zhimenda station from the Yangtze River Conservancy Commission were used to determine runoff from the SRYR (1957–2013). Stations used for these analyses are listed in Table 1 with geographic and climatic information. The Shuttle Radar Topography Mission (SRTM) 90 m digital elevation data was downloaded from the Consortium for Spatial Information (CGIAR-CSI).

Table 1. Hydro-climatic stations used in the analysis.

Station	Longitude	Latitude	Elevation (m)	Mean Annual Temp. (°C)	Mean Annual Precip. (mm)	Thiessen Weight
Temperature and Precipitation						
Wudaoliang	93.08	35.22	4612	−5.3	288.7	0.217
Tuotuohe	92.43	34.22	4533	−3.9	289.4	0.416
Qumalai	95.78	34.13	4175	−2.0	414.2	0.188
Yushu	97.02	33.02	3717	3.4	486.2	0.028
Qingshuihe	97.08	33.48	4415	−4.5	516.7	0.028
Geermu	94.90	36.42	2808	5.2	42.2	0.025
Zaduo	95.30	32.90	4066	0.7	358.8	0.040
Naqu	92.07	31.48	4507	−1.1	292.0	0.003
Suoxian	93.78	31.89	4023	1.9	380.6	0.056
Runoff						
Zhimenda	97.22	33.03		−2.9	327.4	

2.2. Methods

2.2.1. Trend Analysis

Linear trend analysis [22] through simple regression was used to investigate long-term changes in the historical data. The gradient for a long-term changing trend y was estimated as

$$\frac{dy(t)}{dt} = a_1 \quad (1)$$

where a_1 is the linear hydro-climatic trend for one year. The sum of squared residuals (difference between observed and fitted values) was minimized to estimate a_1 .

Nonparametric Mann-Kendall test was selected to examine trends of hydrological and meteorological time series. The method has been widely used in hydro-climatic time series analysis for identifying trends [23,24]. The Mann-Kendall test is independent of the statistical distribution of the data. The statistical significance of the trend was evaluated at the 0.05 level of significance against the null hypothesis that there is no trend for the data series.

2.2.2. Water Balance and Uncertainty Analysis

As evaporation is an important but non-observed variable in water balance analysis, temperature and precipitation data was used to calculate actual evapotranspiration (ET_a) by use of the Takahashi equation [25]:

$$ET_{a_m} = f(P_m, T_m) = \frac{3100P_m}{A + B * P_m^2 \exp\left(-\frac{34.4T_m}{235+T_m}\right)} \quad (2)$$

$$ETa = \sum_{m=1}^{12} ETa_m \quad (3)$$

where ETa = annual actual evapotranspiration (mm), ETa_m = monthly actual evapotranspiration (mm), P_m = monthly precipitation (mm), T_m = mean monthly temperature ($^{\circ}$ C), and A, B = parameters that depend on local meteorological and hydrological conditions. Equations (2) and (3) have previously been tested in the SRYR [21,26] and A and B were determined to 3100 and 0.55 by wavelet and water balance analysis.

Monthly water balances were calculated according to:

$$P_m - ETa_m - R_m = \Delta W_m \quad (4)$$

where P_m = monthly precipitation (mm), ETa_m = monthly actual evapotranspiration (mm), R_m = monthly runoff depth (mm), and ΔW_m = monthly water storage change (mm). Annual water storage change ΔW (mm) was conducted by summation of monthly water storage change.

Water balance calculations are subject to different sources of errors, both from measurement and calculation. To estimate errors, we quantified 10-year moving averages and uncertainties (\pm standard deviation, Std) for different components in the long-term water balance. The upper/lower boundaries were analyzed by adding/subtracting the standard deviations to/from the moving averages. Since water storage change is dependent on temperature, precipitation, and runoff, the standard deviations $Std_{\Delta W}$ were propagated from the independent variables T_m, P_m, R_m according to the formulae below. Standard deviations of T_m, P_m, R_m were calculated using a 10-year moving average window from observed time series [27].

$$Std_{ETa_m} = \sqrt{\left(\frac{\partial f}{\partial T_m}\right)^2 Std_{T_m}^2 + \left(\frac{\partial f}{\partial P_m}\right)^2 Std_{P_m}^2} \quad (5)$$

$$Std_{\Delta W_m} = \sqrt{Std_{ETa_m}^2 + Std_{P_m}^2 + Std_{R_m}^2} \quad (6)$$

$$Std_{\Delta W} = \sqrt{\sum_{m=1}^{12} Std_{\Delta W_m}^2} \quad (7)$$

In order to further validate this approach, we compared the ETa calculated by Equations (2) and (3) and ET' calculated from Langbein's [28] and Turc's empirical relationships [29]. These relationships have been applied to different cold region catchments worldwide for estimating average annual actual evapotranspiration [27,30,31]:

$$PET = 325 + 21T + 0.9T^2 \quad (8)$$

$$ET' = \frac{P}{\sqrt{(0.9 + \left(\frac{P^2}{PET^2}\right))}} \quad (9)$$

where PET = Langbein's potential annual evapotranspiration (mm), T = mean annual temperature ($^{\circ}$ C), ET' = Turc's actual annual evapotranspiration (mm), and P = annual precipitation (mm).

2.2.3. Correlation Analysis

Correlation analysis was used to examine the strength of the relationship between the hydro-climatic variables. Pearson product-moment correlation (R) was used for this purpose [32] and the statistical significance level was set to 95% probability level.

To find potential abrupt changes in climatic time series and compare correlations before and after the change, Change-Point Analyzer [33,34] was used to detect change points. Change-Point Analyzer

is a software package for analyzing time ordered data to determine whether a change has taken place, and it detects multiple changes and provides confidence levels for each of these.

3. Results

3.1. Basic State of Climatic Variables

Locations of the nine hydro-climatic stations are depicted in Figure 1. Figure 2 shows the spatial distribution of annual average hydro-climatic variables (MAT = mean annual temperature, MAP = mean annual precipitation, and CAE = calculated mean annual evapotranspiration (CAE)).

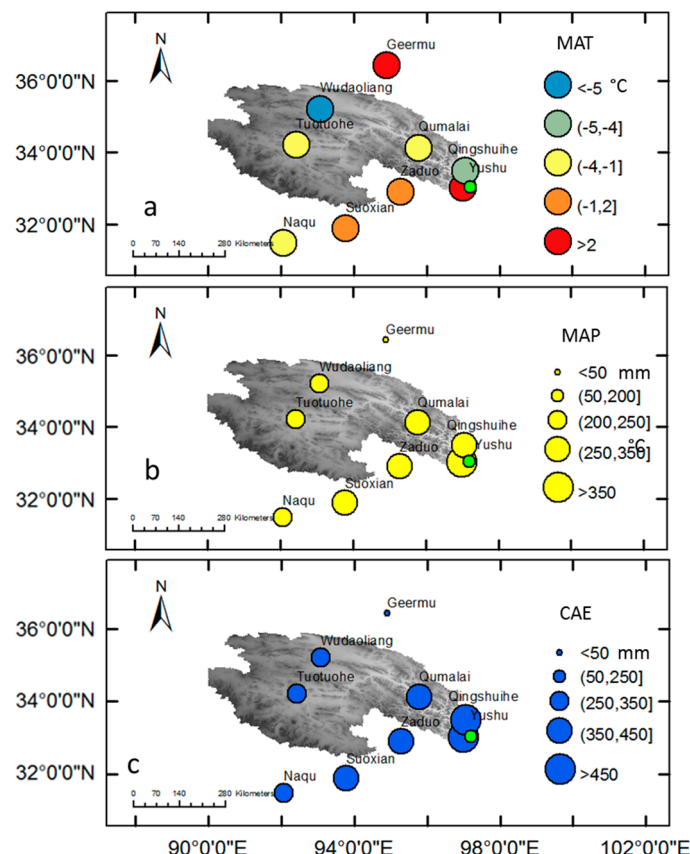


Figure 2. Spatial distribution of annual average hydro-climatic variables in source region of the Yangtze River (SRYR) (1957–2013); (a) mean annual temperature in $^{\circ}\text{C}$; (b) mean annual precipitation in mm; and (c) calculated mean annual evapotranspiration in mm.

Due to the high elevation of the SRYR, the climate is cold, with an annual average temperature of about $-2.9\text{ }^{\circ}\text{C}$ and a range of $-5.5\text{--}3\text{ }^{\circ}\text{C}$ depending on the spatial location (Figure 2a). In Figure 2a, MAT is shown where no simple spatial trend can be observed. In general, however, the north is the part with the lowest temperature inside the watershed.

Located in a highland sub-frigid climate that is semiarid to semi-humid, warm moist air flowing from the Bay of Bengal gives the SRYR an annual average precipitation of 327.4 mm (Figure 2b, Table 2). Most of the region is below the threshold annual precipitation of 400 mm that can be classified as semiarid climate, while the southeast part corresponds to semi-humid [35]. The mean annual precipitation is increasing from northwest to southeast.

The calculated annual mean actual evapotranspiration (CAE) in the SRYR corresponds to 240.3 mm. As seen from the figure the northwestern area has the lowest annual evapotranspiration that

increases to southeast (Figure 2c). The evapotranspiration from May to September (208.7 mm/year) accounts for about 86% of the annual evapotranspiration (240.3 mm/year).

3.2. Temporal Trends

Based on area weights of the Thiessen polygons (Table 1), basin-averaged annual time series were obtained for each variable. Figure 3 shows annual and decadal time series of investigated variables (temperature, precipitation, and runoff; 1957–1990, 1991–2000, 2001–2010, and the latest 10 available years 2004–2013). Table 2 shows the changing gradients and results of the Mann-Kendall test for all investigated variables.

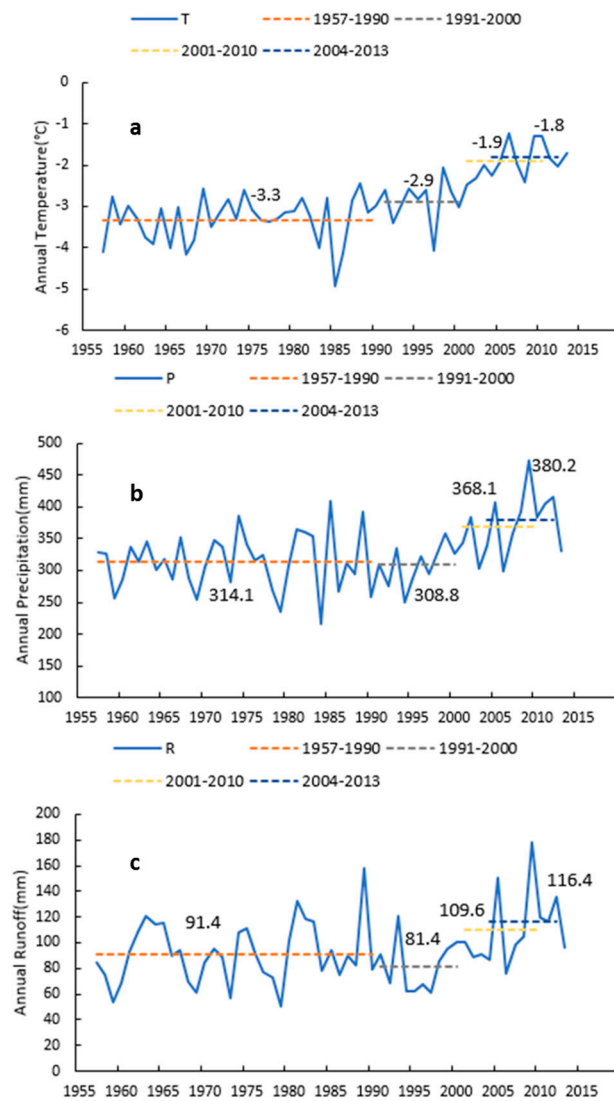


Figure 3. Annual time series and decadal average values for investigated hydro-climatic variables in the SRYR (1957–2013); (a) mean annual temperature in °C; (b) mean annual precipitation in mm; (c) mean annual runoff in mm. Four periods for decadal average: 1957–1990; 1991–2000; 2001–2010; 2004–2013 during the latest 10 years.

Table 2. Trend analysis for investigated hydro-climatic variables in the SRYR.

Trend Analysis Indices	Temperature	Precipitation	Run-Off	Evapotranspiration	Change in Water Storage
Gradient	0.34 (°C/decade)	11.4 (mm/decade)	3.3 (mm/decade)	7.6 (mm/decade)	-1.1 (mm/decade)
MK Sig.	0.000 *	0.004 *	0.077	0.000 *	0.156

Notes: MK Sig. refers to the significant level of each variable in Mann-Kendall test. * Statistically significant at 0.05, 0.000 refers to significant level <0.001.

Long-term trends for temperature and precipitation are positive and statistically significant with an increase of 0.34 °C and 11.4 mm per decade. The runoff displays a small decadal increase by 3.3 mm. However, this is not statistically significant (Table 2). The results for temperature and runoff confirm previously found trends for the study area. A difference, however, is more rapid changes [36–38]. The increasing runoff is statistically significant at 10% level. Annual precipitation in the SRYR was suggested to have non-significant trend for the period 1948–2003 [39] and an increasing but non-significant trend during 1960–2010 [40]. The difference in results is caused by the varying length of time series. The annual precipitation during 2010–2013 has displayed comparably high values and this has an important impact for the entire trend estimation. The decadal mean values after 1990 all display a strong increase as compared to the reference period 1957–1990. All investigated hydro-climatic variables display the highest decadal value during the latest 10-year period. Annual temperature shows a continuously warming trend for the consecutive decadal periods (Figure 3a). Annual runoff had a decline in 1990s but then rebounded in the 2000s and continued to increase which was consistent with the trend of precipitation during this period (Figure 3b,c). The decline in the 1990s has previously been confirmed [7] using data from 1960 to 2000.

3.3. Water Balance and Uncertainty Analysis

To verify the calculation of actual evapotranspiration by the Takahashi formula, a comparison with calculated evapotranspiration using Equations (8) and (9) was done. The mean annual calculated evapotranspiration using these two approaches was 240.3 and 222.4 mm, respectively, with a relative error of 7.4%. These time series are shown in Figure 4a; they display a similar trend. The coefficient of determination between the annual actual evapotranspiration using these two approaches ($R^2 = 0.822$) shows that there is a strong agreement in the results (Figure 4b). Calculated evapotranspiration from the Takahashi formula showed a positive and statistically significant trend of 7.6 mm per decade since it is calculated essentially from temperature and precipitation, which also show a clear increase (Table 2).

Annual water storage change (ΔW) was calculated based on water balance. It shows a small but insignificant negative trend (MK Sig. 0.156 > 0.05, Table 2). Annual time series and uncertainty boundaries are shown in Figure 5. The basin scale water storage with the 10-year moving average for ΔW is generally below zero, which indicates that the basin is losing water storage (Figure 5). However, considering the uncertain boundaries propagated from the observation components and calculation process, the true water storage change can also be close to zero or positive. To summarize, the basin as a whole does not display a significant loss of water storage, although the 10-year average basin-scale water balance indicates a continuous small negative value since about 1980. In this case, the increase of calculated evapotranspiration derived from significantly increasing temperature, together with an increase in precipitation, leads to a relatively stable water storage during the study period.

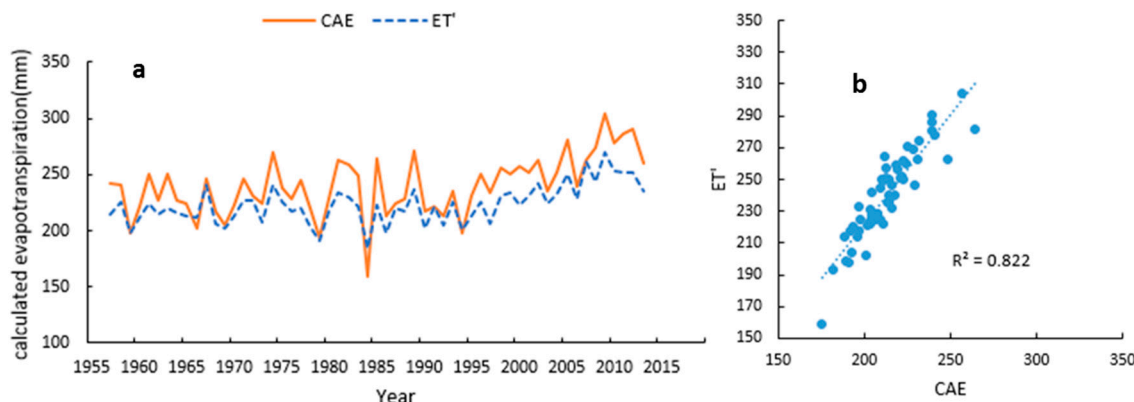


Figure 4. Correlation between CAE (Takahashi) and ET' (L-T); (a) time series of calculated annual evapotranspiration (CAE as solid line, ET' as dashed line) in mm; (b) cross correlation between CAE and ET' .

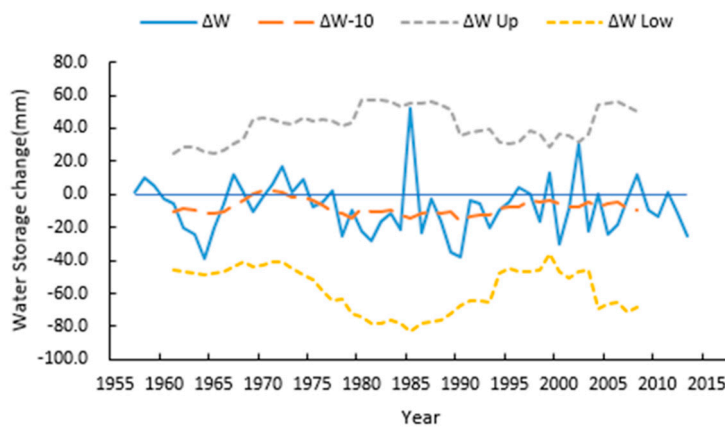


Figure 5. Annual time series for water storage change in SRYR; Annual time series of ΔW , 10-year moving average as $\Delta W-10$, upper and lower uncertainty boundaries as ΔW Up/Low.

3.4. Correlation between Hydro-Climatic Variables

Runoff from the SRYR is supplied by either direct precipitation or melt water from ice and snow, and groundwater [37]. The annual distribution of runoff thus changes with precipitation and temperature conditions. Generally, during November to April, the rivers are frozen, and in May the ice begins to melt, displaying a small discharge. The river discharge increases until July, when a maximum occurs.

To estimate the correlation between runoff and climatic variables, analysis was conducted both at annual and monthly scale (1957–2013). Annual runoff is strongly correlated with precipitation ($R = 0.80$; statistically significant at the 5% level) but less with temperature ($R = 0.26$). The correlation indicates the dominant role of precipitation during runoff generation in the SRYR. Figure 6 shows the correlation between monthly temperature, precipitation, and runoff. A statistically significant positive correlation between precipitation and runoff from May to October (1% level) can be observed. However, in the cold season (November to April), the most significant influencing factor is temperature (0.05 level).

As climate is undergoing a rapid change, especially in recent decades, correlation between variables will also change. The entire time series was divided into two periods (1957–1990, 1991–2013), with changing points included in the second period. Correlation between precipitation, temperature, and runoff are shown for both periods in Figure 7. Change point analyzer showed that annual temperature and precipitation have a changing point at 1997 and 2004, with 99% and 95% significance

levels respectively. As seen from Figure 7a, the relative influence from temperature increased during the second period. A similar change for precipitation did not occur. A specific change for precipitation was observed for the winter period in Figure 7b. The correlation between precipitation and runoff varied around zero from November to April in both periods, and even had negative values in period 2, which indicate a weak influence from precipitation on winter runoff. This is consistent with the enhanced influence of temperature in winter.

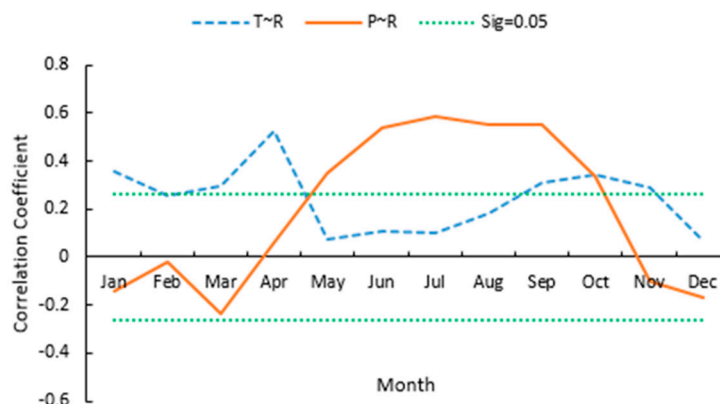


Figure 6. Correlation between monthly precipitation and runoff and temperature and runoff in SRYR; T-R is correlation between temperature and runoff depicted by a dashed blue line; P-R is correlation between precipitation and runoff depicted as solid orange line; significance level 0.05 is depicted as green dot line, positive correlation above green line is statistically significant.

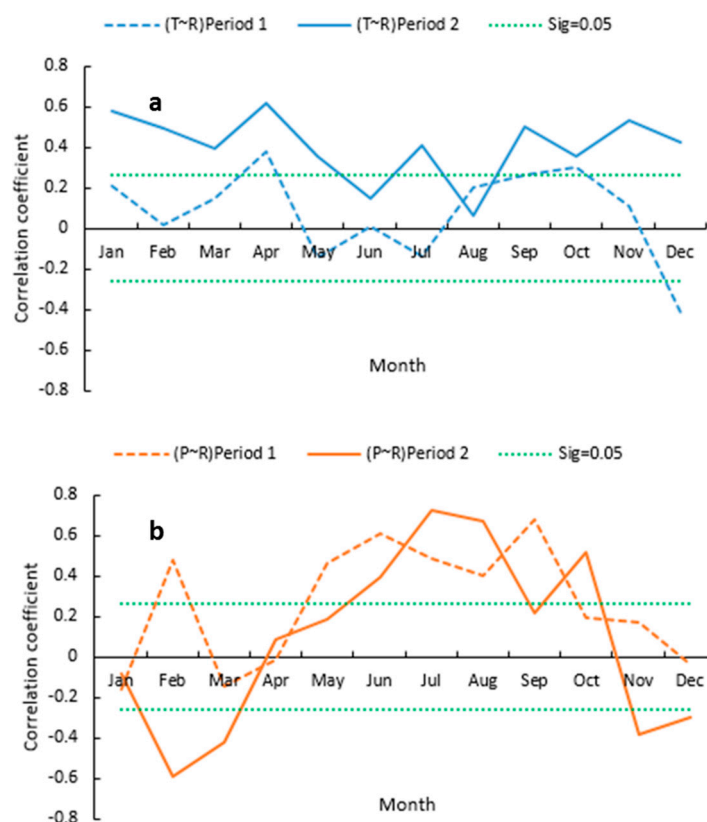


Figure 7. Correlation between monthly precipitation and runoff and temperature and runoff; (a) 1957–1990 (period 1); (b) 1991–2013 (period 2); significance level 0.05 is shown as a green dot line, positive correlation above and negative correlation below green line are statistically significant.

There are many possible reasons for the enhancing or decreasing correlation between climatic variables and runoff. For example, permafrost degradation and glacial melt can reflect and strengthen the influence of temperature in spring. However, to validate these interactions for the hydrological cycle, more observations and measurements are necessary. Gravity Recovery and Climate Experiment (GRACE) datasets provide a new way to estimate the land water content [41]. Meanwhile, research can also analyze both long-term averages and extreme events of runoff to find indicators of dominate influence factors using daily/hourly data.

4. Conclusions

Analysis of hydro-climatic components of the SRYR using the most recent data was done. Correlation analysis between climate variables and runoff was developed. Based on the results, the main conclusions of this study are:

- (1) The temperature in the SRYR increased at a rate of 0.34 °C/decade, and the precipitation and evaporation also increased by 11.4 and 7.6 mm/decade, respectively. The runoff depth increased by 3.3 mm/decade;
- (2) The annual water storage change appears stable. However, it displays a continuous small negative trend. Based on water balance equation, the increase in calculated evapotranspiration derived from significantly increasing temperature and precipitation lead to relatively stable water storage during the study period;
- (3) Temperature is the dominating factor for runoff during the cold season (November to April) and precipitation for the runoff during the warm season (May to October). Temperature appears to have increased as a dominating factor during the recent 1991–2013 period as compared to the period 1957–1990. Decreasing correlation between precipitation and runoff also indicates the enhancing influence of temperature on runoff in winter.

Acknowledgments: Funding from the National Key Research Projects (Grant No. 2016YFC0402704) and the National Natural Science Foundation of China (Grant No. 41371047) are gratefully acknowledged. Support from the China Postdoctoral Science Foundation (Grant No. 2016M601711) and the Jiangsu Planned Projects for Postdoctoral Research Funds (Grant No. 1601027B) are appreciated. The first author also acknowledges support from the China Scholarship Council.

Author Contributions: Yiheng Du planned the research with co-authors, performed the analysis, and wrote the paper with the co-authors. Co-authors provided the data, gave advice, and helped to revise the paper.

Conflicts of Interest: The authors declare no conflict of interest.

References

1. Stocker, T.F.; Qin, D.; Plattner, G.K.; Tignor, M.M.B.; Allen, S.K.; Boschung, J.; Nauels, A.; Xia, Y.; Bex, V.; Midgley, P.M. *Climate Change 2013 the Physical Science Basis: Working Group I Contribution to the Fifth Assessment Report of the Intergovernmental Panel on Climate Change*; Cambridge University Press: Cambridge, UK, 2013.
2. Hu, Y.G.; Jiang, L.L.; Wang, S.P.; Zhang, Z.H.; Luo, C.Y.; Bao, X.Y.; Niu, H.S.; Xu, G.P.; Duan, J.C.; Zhu, X.X.; et al. The temperature sensitivity of ecosystem respiration to climate change in an alpine meadow on the Tibet plateau: A reciprocal translocation experiment. *Agric. For. Meteorol.* **2016**, *216*, 93–104. [[CrossRef](#)]
3. Wu, Q.; Dong, X.; Liu, Y.; Jin, H. Responses of permafrost the qinghai-tibet plateau, China, to climate change and engineering construction. *Arct. Antarct. Alp. Res.* **2007**, *39*, 682–687. [[CrossRef](#)]
4. Liu, Z.F.; Yao, Z.J.; Wang, R. Contribution of glacial melt to river runoff as determined by stable isotopes at the source region of the Yangtze River, China. *Hydrol. Res.* **2016**, *47*, 442–453. [[CrossRef](#)]
5. Yao, T.D.; Liu, X.D.; Wang, N.L.; Shi, Y.F. Amplitude of climatic changes in Qinghai-Tibetan Plateau. *Chin. Sci. Bull.* **2000**, *45*, 1236–1243. [[CrossRef](#)]
6. Liu, S.Y.; Zhang, Y.; Zhang, Y.S.; Ding, Y.J. Estimation of glacier runoff and future trends in the Yangtze River source region, China. *J. Glaciol.* **2009**, *55*, 353–362.
7. Yang, J.P.; Ding, Y.J.; Chen, R.S. Climatic causes of ecological and environmental variations in the source regions of the Yangtze and Yellow Rivers of China. *Environ. Geol.* **2007**, *53*, 113–121. [[CrossRef](#)]

8. Zhang, S.; Hua, D.; Meng, X.; Zhang, Y. Climate change and its driving effect on the runoff in the “Three-River Headwaters” region. *J. Geogr. Sci.* **2011**, *21*, 963–978. [[CrossRef](#)]
9. Bing, L.F.; Shao, Q.Q.; Liu, J.Y. Runoff characteristics in flood and dry seasons based on wavelet analysis in the source regions of the Yangtze and Yellow rivers. *J. Geogr. Sci.* **2012**, *22*, 261–272. [[CrossRef](#)]
10. Chongyi, E.; Hu, H.; Xie, H.; Sun, Y. Temperature change and its elevation dependency in the source region of the Yangtze River and Yellow River. *J. Geogr. Geol.* **2014**, *6*, 124–131.
11. Kang, S.; Zhang, Y.; Qin, D.; Ren, J.; Zhang, Q.; Grigholm, B.; Mayewski, P.A. Recent temperature increase recorded in an ice core in the source region of Yangtze River. *Chin. Sci. Bull.* **2007**, *52*, 825–831. [[CrossRef](#)]
12. Yao, Z.J.; Liu, Z.F.; Huang, H.Q.; Liu, G.H.; Wu, S.S. Statistical estimation of the impacts of glaciers and climate change on river runoff in the headwaters of the Yangtze River. *Quat. Int.* **2014**, *336*, 89–97. [[CrossRef](#)]
13. Wu, S.S.; Yao, Z.J.; Huang, H.Q.; Liu, Z.F.; Chen, Y.S. Glacier retreat and its effect on stream flow in the source region of the Yangtze River. *J. Geogr. Sci.* **2013**, *23*, 849–859. [[CrossRef](#)]
14. Fang, Y.P.; Qin, D.H.; Ding, Y.J. Frozen soil change and adaptation of animal husbandry: A case of the source regions of Yangtze and Yellow Rivers. *Environ. Sci. Policy* **2011**, *14*, 555–568. [[CrossRef](#)]
15. Duo, B.; Bianbaciren; Li, L.; Wang, W.; Zhaxiyangzong. The response of lake change to climate fluctuation in north Qinghai-Tibet Plateau in last 30 years. *J. Geogr. Sci.* **2009**, *19*, 131–142.
16. Huang, L.; Liu, J.Y.; Shao, Q.Q.; Liu, R.G. Changing inland lakes responding to climate warming in Northeastern Tibetan Plateau. *Clim. Chang.* **2011**, *109*, 479–502. [[CrossRef](#)]
17. Xiang, L.W.; Wang, H.S.; Steffen, H.; Wu, P.; Jia, L.L.; Jiang, L.M.; Shen, Q. Groundwater storage changes in the Tibetan Plateau and adjacent areas revealed from GRACE satellite gravity data. *Earth Planet. Sci. Lett.* **2016**, *449*, 228–239. [[CrossRef](#)]
18. Liu, S.Y.; Sun, W.X.; Shen, Y.P.; Li, G. Glacier changes since the Little Ice Age maximum in the western Qilian Shan, northwest China, and consequences of glacier runoff for water supply. *J. Glaciol.* **2003**, *49*, 117–124.
19. Zhang, M.F.; Ren, Q.S.; Wei, X.H.; Wang, J.S.; Yang, X.L.; Jiang, Z.S. Climate change, glacier melting and streamflow in the Niyang River Basin, Southeast Tibet, China. *Ecohydrology* **2011**, *4*, 288–298. [[CrossRef](#)]
20. Barnett, T.P.; Adam, J.C.; Lettenmaier, D.P. Potential impacts of a warming climate on water availability in snow-dominated regions. *Nature* **2005**, *438*, 303–309. [[CrossRef](#)] [[PubMed](#)]
21. Qian, K.; Wang, X.-S.; Lv, J.; Wan, L. The wavelet correlative analysis of climatic impacts on runoff in the source region of Yangtze River, in China. *Int. J. Climatol.* **2014**, *34*, 2019–2032. [[CrossRef](#)]
22. Kenney, J.F.; Keeping, E.S. Linear Regression and Correlation. *Math. Stat.* **1951**, *8*, 199–237.
23. Burn, D.H.; Elnur, M.A.H. Detection of hydrologic trends and variability. *J. Hydrol.* **2002**, *255*, 107–122. [[CrossRef](#)]
24. Yuan, F.F.; Berndtsson, R.; Zhang, L.; Uvo, C.B.; Hao, Z.C.; Wang, X.P.; Yasuda, H. Hydro Climatic Trend and Periodicity for the Source Region of the Yellow River. *J. Hydrol. Eng.* **2015**, *20*, 05015003. [[CrossRef](#)]
25. Takahashi, K.; Wang, C.G. The projection formula for evapotranspiration from the monthly mean temperature and monthly precipitation. *Meteorol. Sci. Technol.* **1979**, *26*, 29–32. (In Chinese)
26. Zhang, G.S.; Shi, X.H.; Li, D.L.; Wang, Q.C.; Dai, S. Climate change in Tuotuohe Area at the headwaters of Yangtze River. *J. Glaciol. Geocryol.* **2006**, *28*, 678–685. (In Chinese)
27. Karlsson, J.M.; Lyon, S.W.; Destouni, G. Thermokarst lake, hydrological flow and water balance indicators of permafrost change in Western Siberia. *J. Hydrol.* **2012**, *464*, 459–466. [[CrossRef](#)]
28. Langbein, W.B. *Annual Runoff in the United States*; US Geological Survey Circular: Reston, VA, USA, 1949; p. 54.
29. Turc, L. Estimation of irrigation water requirements, potential evapotranspiration: A simple climatic formula evolved up to date. *Ann. Agron.* **1961**, *12*, 13–49.
30. Tabari, H. Evaluation of Reference Crop Evapotranspiration Equations in Various Climates. *Water Resour. Manag.* **2010**, *24*, 2311–2337. [[CrossRef](#)]
31. Federer, C.A.; Vorosmarty, C.; Fekete, B. Intercomparison of methods for calculating potential evaporation in regional and global water balance models. *Water Resour. Res.* **1996**, *32*, 2315–2321. [[CrossRef](#)]
32. Pearson, K. Mathematical Contributions to the Theory of Evolution. III. Regression, Heredity, and Panmixia. *Philos. Trans. R. Soc. Lond.* **1896**, *187*, 253–318. [[CrossRef](#)]
33. Taylor, W.A. Change-Point Analysis: A Powerful New Tool for Detecting Changes. Available online: <http://www.variation.com/cpa/tech/changepoint.html> (accessed on 10 February 2017).

34. Yuan, F.; Hao, Z.; Berndtsson, R.; Jiang, P.; Yasuda, H. The Mass Balance of Glacier No. 1 at the Headwaters of the Urumqi River in Relation to Northern Hemisphere Teleconnection Patterns. *Water* **2016**, *8*, 100. [[CrossRef](#)]
35. Gao, J.B.; Huang, J.; Li, S.C.; Cai, Y.L. The New Progresses and Development Trends in the Research of Physio-Geographical Regionalization in China. *Prog. Geogr.* **2010**, *29*, 1400–1407. (In Chinese)
36. Xie, C.W.; Ding, Y.J.; Liu, S.Y.; Wang, G.X. Comparison Analysis of Runoff Change in the Source Regions of the Yangtze and Yellow Rivers. *J. Glaciol. Geocryol.* **2003**, *25*, 414–422. (In Chinese)
37. Liang, C.; Hou, X.B.; Pan, N. Spatial and temporal variations of precipitation and runoff in the source region of the Yangtze River. *South-to-North Water Divers. Sci. Technol.* **2011**, *9*, 35–39. (In Chinese) [[CrossRef](#)]
38. Li, L.; Shen, H.Y.; Dai, S.; Li, H.M.; Xiao, J.S. Response of water resources to climate change and its future trend in the source region of the Yangtze River. *J. Geogr. Sci.* **2013**, *23*, 208–218. [[CrossRef](#)]
39. Wang, K.L.; Cheng, G.D.; Ding, Y.J.; Shen, Y.P.; Jiang, H. Characteristics of water vapor transport and atmospheric circulation of precipitation over the source regions of the Yellow and Yangtze Rivers. *J. Glaciol. Geocryol.* **2006**, *28*, 8–14. (In Chinese)
40. Li, S.S.; Zhang, M.J.; Wang, B.L.; Li, X.F.; Luo, S.F. Spatial difference of precipitation variation in Three-River headwaters region of China in recent 51 years. *Chin. J. Ecol.* **2012**, *31*, 2635–2643. (In Chinese)
41. Wahr, J.; Swenson, S.; Zlotnicki, V.; Velicogna, I. Time-variable gravity from GRACE: First results. *Geophys. Res. Lett.* **2004**, *31*, L11501. [[CrossRef](#)]



© 2017 by the authors; licensee MDPI, Basel, Switzerland. This article is an open access article distributed under the terms and conditions of the Creative Commons Attribution (CC BY) license (<http://creativecommons.org/licenses/by/4.0/>).